Determination of the nuclear level density at high excitation energy

A. Chbihi, L. G. Sobotka, N. G. Nicolis, D. G. Sarantites, D. W. Stracener, and Z. Majka*
Department of Chemistry, Washington University, St. Louis, Missouri 63130

D. C. Hensley, J. R. Beene, and M. L. Halbert
Oak Ridge National Laboratory, Oak Ridge, Tennessee 37830
(Received 12 July 1990)

Evaporation simulations are presented to illustrate the problems associated with the determination of the nuclear level density constant at high excitation energy from evaporation spectra. The methods of using either the total (whole chain) spectra or the difference (from two different initial excitation energies) spectra are discussed. Data from the study of the reaction 701 MeV $^{28}Si+^{100}Mo$ are presented and both methods are used to extract the level density constant. We find that in order to reproduce the slopes of the light particle spectra the level density constant must have a value near $\frac{1}{10}A-\frac{1}{11}A$ for excited nuclei with statistical temperatures in the range of 3.5 to 5.5 MeV. This presumes that the only parameter adjustment required to treat the decay of highly exited nuclei is the level density constant. If this is so, the shapes of the evaporation spectra imply a reduction in the level density constant from the value required to explain the decay of less highly excited nuclei, a conclusion reached by others. However, the reduced level density constant leads to an overproduction of deuterons and tritons. This suggests that a more complicated set of parameter adjustments may be required to treat the decay of highly excited nuclei.

I. INTRODUCTION

One of the most exciting opportunities opened by heavy-ion reactions is the possibility of measuring the evolution of the nuclear level density (ρ) to very high excitation energies. At moderate excitation energy, we have been guided by the Fermi gas dependence,[1]

$$\rho(U)\propto\frac{g_0}{(g_0U)^{5/4}}\exp\left[2\left[\frac{\pi^2}{6}g_0U\right]^{1/2}\right]. \tag{1}$$

The equation of state implied by Eq. (1) is

$$T^{-1}\equiv\frac{1}{\rho}\frac{\partial\rho}{\partial U}=\left[\frac{\pi^2}{6}\frac{g_0}{U}\right]^{1/2}-\frac{5}{4}U^{-1}. \tag{2}$$

The second term can be neglected except in those cases involving either light nuclei or low excitation energy. Dropping the second term yields the familiar expressions

$$U=\left[\frac{\pi^2}{6}g_0\right]T^2=aT^2 \tag{3}$$

and

$$C=2aT \tag{4}$$

for the excitation energy and heat capacity, respectively. In these expressions, U is the excitation energy (above the rotating ground state), and g_0 is the single-particle level density in the region of the Fermi energy (ε_f), and T is the statistical temperature. A uniform Fermi gas model provides the first estimate of the single-particle level density at the Fermi surface and therefore our first estimate of the level density constant a:

$$a=\frac{\pi^2}{6}g_0(\varepsilon_f)=\frac{\pi^2A}{4\varepsilon_f}\approx A/15, \tag{5}$$

where A is the atomic mass number. This simple estimate does yield the experimentally determined mass dependence, but the experimental values of a at low excitation energy are systematically larger than calculated with Eq. (5). There are many reasons to expect the logic behind Eq. (5) to fail. One reason is that it neglects the influence of the diffuse surface region of real nuclei.[2] Another reason is that it neglects the effect of the nuclear medium on the nucleon mass. The effective mass (m^*) of the nucleon can be defined in terms of the single-particle density of states with momentum k,

$$g_0=\frac{dk}{d\varepsilon(k)}=\frac{m^*}{k}. \tag{6}$$

Equation (6) is particularly illustrative because it is known that, in cold nuclei, m^*/m exhibits a peak as a function of k at the Fermi momentum.[3,4] The value of m^*/m at k_f is of the order of 1.3 which in part explains the deviation of the result in (5) from the experimental findings. On the other hand, the enhancement of the effective mass is expected to vanish with excitation energy.[5–7] One would therefore expect the constant a to decrease with excitation energy.

Experimental work, utilizing the shape of evaporation spectra, suggests that the level density constant is reduced at high excitation energy.[8–10] These experimental works provided the motivation to examine the theory relevant to the temperature dependence of the level density constant[5–7] as well as inciting us to examine the issue

from the experimental side. Our approach to this issue is similar to that of the previous experimental work[8–10] in that we utilize the shape of the evaporation spectra; however we also make use of the absolute particle multiplicities. Furthermore, we provide detailed evaporation simulations in order to illustrate the problems associated with the methods for extracting the constant a at high excitation energy.

II. EVAPORATION SIMULATION

A. Background—why simulate

At low excitation energy, the level density constant is determined from the explicit counting of resonances. The deduced values of a exhibit understandable oscillations, due to shell structure, around the value of $\sim A/8.5$. The oscillations are, with very few exceptions, within 15% of this value. (This allows for a variable "back shifting" of the energy to include empirically the influence of odd-even mass differences and shell structure.[11–13])

The level density constants determined at low energy have been extensively used at moderate excitation energies (≤ 100 MeV) in simulations of the evaporation cascade of compound nuclei produced by both light- and heavy-ion bombardments. As an example, we provide a comparison of experimental[14] and calculated p, d, t, and α spectra for the decay of ^{117}Te produced in the reaction 121 MeV ^{14}N+^{103}Rh, in Fig. 1. The calculations were done with the code PACEX.[15] This code increases the number of decay channels over those allowed in the old version of PACE (new version includes n, p, d, t, ^{3}He, ^{4}He, and ^{6}Li), allows excitation energies up to 600 MeV, calculates transmission coefficients for each element in the cascade, and contains additional options for the calculation of the level density. The important parameters for this system and the other systems considered in this paper are given in Table I. The evaporation simulation, shown in Fig. 1 (thin curves) for the ^{14}N+^{103}Rh system, uses a Fermi gas level density form[16] with a level density parameter and backshift which vary from nucleus to nucleus.[12] The

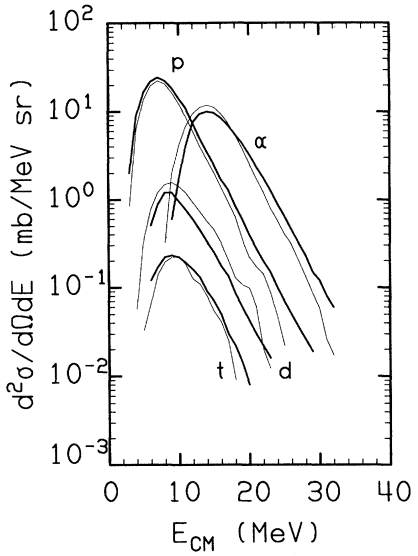

FIG. 1. Comparison of experimental (thick curves) and PACEX evaporation simulations (thin curves) of the p, d, t, and α-particle spectra for the decay of ^{117}Te produced in the reaction 121 MeV ^{14}N+^{103}Rh.

level density parameters are in the range of $A/7$ to $A/9$ (Ref. 12). Furthermore, at these moderate excitation energies, attention must be paid to the form of the spin distribution[17] and the rotational energy. The rotational energy is calculated using moments of inertia calculated with a finite range corrected liquid drop model.[18] These rotational inertias are expected to be appropriate for either moderate to high excitation energy or high spin, where the affect of pairing on the inertia is gone. These calculations reproduce the cross sections to within 30%, and the shapes of the energy spectra for protons, deuterons, and tritons as well as the α-particle cross section. The less than perfect simulation of the shape of the α-particle spectrum is likely due to deficiencies in the treat-

TABLE I. Relevant parameters of the simulated reactions.

System	CN	E^* [a] (MeV)	l ($\hbar$)	$k \equiv A/a$ (MeV)	Simulation for bin no.
(1) 121 MeV ^{14}N+^{103}Rh	^{117}Te	106	52[b]	From Ref. 12 with equation from Ref. 16	
(2) 200 MeV ^{10}B+^{100}Mo	^{110}Ag	198	0 and 53[b]	8.5,11	
(3) 261 MeV ^{10}B+^{100}Mo	^{110}Ag	253	0 and 53[b]	8.5,11	
(4) 152 MeV ^{6}Li+^{100}Mo	^{106}Rh	158	18.2[c]	6,8.5,11	1
(5) 197 MeV ^{7}Li+^{100}Mo	^{107}Rh	200	21.1[c]	6,8.5,11	2
(6) 271 MeV ^{10}B+^{100}Mo	^{110}Ag	260	27.2[c]	6,8.5,11	3
(7) 354 MeV ^{14}N+^{100}Mo	^{114}In	316	36.1[c]	6,8.5,11	4
(8) 441 MeV ^{19}F+^{100}Mo	^{119}Sb	372	47.7[c]	6,8.5,11	5
(9) 494 MeV ^{21}Ne+^{100}Mo	^{121}Te	405	48.8[c]	6,8.5,11	6

[a]Initial excitation energy.
[b]Critical angular momentum for fusion. If l is nonzero, the value was calculated with the Bass model (Ref. 17).
[c]The average angular momentum estimated from the sum-rule model.

ment of the rotational energy. This problem becomes even more severe in the simulation of the decay of compound nuclei formed with even lower excitation energy but large angular momentum. In these cases, the yrast structure and perhaps even the near yrast structure[19] as well as the gamma strengths are important.

At higher excitation energies, one must also rely on a comparison of experimental evaporation spectra and statistical model calculations to provide the basis on which to evaluate nuclear level densities. While one might be tempted to use Eq. (3) directly with a temperature deduced from fitting the evaporation spectra and an estimate of the daughter excitation energy, this leads to large errors. The slopes of evaporation spectra can only be related to the statistical temperature [defined by Eq. (2)] after consideration of the competition between decay channels along the cascade. In the work of Hilscher *et al.*,[8] this complication was dealt with my multiplying the slopes of the evaporation spectra by correction factors, (f_w). The correction factors were determined from statistical model calculations, and were those required to obtain a known daughter excitation energy (U_d) from the input level density parameter and the fitted slopes (S)

$$U_d = a(f_w S)^2 \ . \tag{7}$$

Another procedure to deduce a is to use the difference spectra (from the difference of spectra at two different initial excitation energies) to get a temperature corresponding to a small region of excitation energy. This technique was used by Gonin *et al.*[10] It removes the influence of the long evaporation chain on the correction factors, and thus the factors are much closer to unity. However, they still must be estimated with statistical model simulations due to the competition between the decay channels in the angular momentum degree of freedom. (There may also be some remaining competition along the decay chain, if the excitation energy step is large.) We employ both of these procedures and use statistical model calculations to show how these correction factors, f_w for correcting the slopes of spectra resulting from the whole cascade and f_d for correcting the slopes resulting from difference spectra, vary with evaporation channel, excitation energy, and angular momentum.

The discussion above outlines two methods which utilize the shape of evaporation spectra, in particular the slope, to provide information on the level density constant. However, the value of the level density constant also has a direct influence on the particle multiplicities. The yield of all channels which substantially reduce the excitation energy of the compound system are enhanced with a reduced level density constant. Therefore reducing a, increases the slope parameter of the Maxwellian spectral shape and increases the multiplicity of the channels with large negative Q values, such as deuteron and triton emission. Therefore, in our quest to study the level density constant at high excitation energy, we not only look at the shape of evaporation spectra but also at the particle multiplicities of the decay channels.

B. Test cases

In order to determine how to correct spectra so that Eq. (7) can be used to determine the level density parameter, we have performed statistical model calculations for the system $^{10}B+^{100}Mo$. (This system is similar to the experimental incomplete fusion reaction discussed in the next section.) A total of six calculations were done; all combinations of two energies, two spin distributions (zero spin and the complete fusion spin distribution with the critical angular momentum determined by the Bass model[17]), and two level density parameters ($A/8.5$ and $A/11$). The evaporation spectra for charged particles were fitted with a surface Maxwellian form shifted by the Coulomb barrier (Cb),

$$\frac{d\sigma}{dE} \propto [E-(\mathrm{Cb})]\exp\{-[E-(\mathrm{Cb})]/S\} \ . \tag{8a}$$

and for neutrons with a volume Maxwellian form,

$$\frac{d\sigma}{dE} \propto E^{1/2}\exp(-E/S) \ . \tag{8b}$$

The slope factors (S) are related to the statistical temperatures through the correction factors. The thermal energy of the primary daughter was calculated as

$$U_d = E^* - (BE) - \bar{\epsilon} - \bar{E}_r \ , \tag{9}$$

where E^* is the initial excitation energy, (BE) is the binding energy of the particle emitted, $\bar{\epsilon}$ is the average channel energy, and $\bar{E}_r$ is the average rotational energy. The root-mean-square spin value and rigid sphere moments of inertia are used to calculate $\bar{E}_r$. The values of S [from Eq. (8)], U_d [from Eq. (9)], a (input to the simulation) are used directly in Eq. (7) to deduce the whole cascade correction factors f_w. All important numbers are given in Table II and the values of f_w are plotted, for the 198 and 254 MeV excitation energies, in Figs. 2(a) and 2(b), respectively.

The two most obvious observations that can be made from inspecting Fig. 2 are that the factors are greater than 1 and that they seem to be rather insensitive to the value of a. The large values of f_w simply reflect the fact that the spectra are the result of summing contributions from all portions of the cascade and that we are correcting up to an energy corresponding to the first chance daughter. The second observation assures us that we can apply these correction factors to experimental data, where the value of a is not known, as long as the parameters other than a are known.

The influence of a spin distribution is also clearly illustrated in Fig. 2. The divergence of the values for the zero initial spin calculations versus those for the spin distribution calculations with increasing ejectile mass indicates that the heavier evaporated particles are more sensitive to the details of the spin distribution. This suggests that unless the spin distribution is well known, one should avoid drawing conclusions based on α-particle spectra using this method. (Bear in mind that a 10% uncertainty in f_w propagates into a 20% uncertainty in a.) The relative decrease of the values of f_w, with increasing evaporated particle mass, in the case with a spin distribution versus the case with zero spin can be understood as an increase

TABLE II. Whole spectra correction factors for the system $^{10}B+^{100}Mo$.

Part.	M [a]	S [b] (MeV)	$\bar{\epsilon}$ [c] (MeV)	A [d]	U_d [e] (MeV)	f_w [f]
			(a) $k=A/a=8.5$ MeV			
Zero initial spin						
$E^*=254$ MeV						
n	11.30	3.48(0.10)	5.4	109	242	1.25(0.02)
p	2.75	3.54(0.15)	10.6	109	236	1.22(0.05)
α	0.94	2.87(0.13)	16.0	105	235	1.52(0.07)
d	0.91	3.24(0.10)	11.6	108	231	1.32(0.05)
t	0.30	3.10(0.10)	11.0	107	229	1.38(0.05)
($E^*=198$ MeV						
n	9.98	3.11(0.08)	5.0	109	186	1.23(0.04)
p	2.05	3.18(0.14)	10.0	109	181	1.18(0.05)
α	0.75	2.78(0.10)	15.3	105	179	1.37(0.05)
d	0.58	3.10(0.20)	11.0	108	176	1.20(0.08)
t	0.18	2.60(0.40)	10.6	107	173	1.43(0.22)
Fusion initial angular momentum distribution						
$E^*=254$ MeV						
n	10.54	3.55(0.08)	5.5	109	226	1.18(0.03)
p	2.19	3.62(0.10)	10.8	109	221	1.15(0.04)
α	1.23	3.81(0.10)	17.1	105	218	1.10(0.03)
d	1.03	3.73(0.10)	12.6	108	215	1.10(0.03)
t	0.37	3.92(0.15)	12.6	107	212	1.05(0.04)
$E^*=198$ MeV						
n	9.20	3.19(0.06)	5.0	109	171	1.15(0.03)
p	1.57	3.26(0.14)	10.1	109	166	1.10(0.05)
α	1.01	3.62(0.11)	17.0	105	162	1.00(0.03)
d	0.66	3.42(0.13)	12.0	108	160	1.04(0.04)
t	0.21	3.55(0.15)	12.3	107	156	0.99(0.05)
			(b) $k=A/a=11$ MeV			
Zero initial spin						
$E^*=254$ meV						
n	10.19	3.85(0.10)	6.0	109	241	1.28(0.04)
p	2.38	3.99(0.11)	11.6	109	235	1.22(0.04)
α	1.07	3.30(0.10)	16.0	105	234	1.50(0.05)
d	1.11	3.75(0.08)	12.1	108	231	1.30(0.03)
t	0.44	3.42(0.08)	11.5	107	229	1.42(0.04)
$E^*=198$ MeV						
n	8.98	3.46(0.07)	5.4	109	185	1.25(0.03)
p	1.78	3.66(0.10)	11.0	109	180	1.17(0.04)
α	0.84	2.86(0.14)	16.1	105	179	1.51(0.08)
d	0.73	3.23(0.13)	11.7	108	175	1.30(0.06)
t	0.28	3.17(0.12)	11.1	107	173	1.33(0.05)
Fusion initial angular momentum distribution						
$E^*=254$ MeV						
n	9.30	3.91(0.10)	6.0	109	226	1.22(0.03)
p	1.82	4.09(0.10)	11.8	109	220	1.15(0.03)
α	1.34	4.17(0.12)	18.0	105	217	1.14(0.04)
d	1.22	4.33(0.12)	13.3	108	214	1.08(0.03)
t	0.50	4.44(0.15)	13.6	107	211	1.05(0.04)
$E^*=198$ MeV						
n	8.15	3.49(0.10)	5.4	109	171	1.19(0.04)
p	1.33	3.71(0.10)	11.0	109	165	1.10(0.03)
α	1.22	3.96(0.10)	17.5	105	161	1.04(0.03)
d	0.79	3.85(0.12)	12.4	108	159	1.05(0.04)
t	0.32	4.00(0.10)	13.0	107	156	1.00(0.03)

TABLE II. (*Continued*).

Part.	M [a]	S [b] (MeV)	$\bar{\epsilon}$ [c] (MeV)	A [d]	U_d [e] (MeV)	f_w [f]
(c) Influence of the backshifting and the other decay channels, Energy = 198 MeV, $k = A/8.5$						
Backshift						
n	9.20	3.19(0.06)	5.0	109	171	1.15(0.03)
p	1.57	3.26(0.14)	10.1	109	166	1.10(0.05)
α	1.01	3.62(0.11)	17.0	105	162	1.00(0.03)
d	0.66	3.42(0.13)	12.0	108	160	1.04(0.04)
t	0.21	3.55(0.15)	12.3	107	156	0.99(0.05)
No backshift						
n	9.70	3.23(0.09)	5.0	109	171	1.13(0.03)
p	1.28	3.23(0.10)	10.0	109	166	1.11(0.04)
α	0.99	3.56(0.13)	17.0	105	162	1.02(0.04)
d	0.59	3.54(0.11)	12.0	108	160	1.00(0.03)
t	0.23	3.69(0.15)	12.0	107	156	0.96(0.04)
Limited set of decay channels (n,p,α only)						
n	10.27	3.29(0.10)	5.1	109	171	1.11(0.04)
p	1.94	3.14(0.10)	10.5	109	166	1.15(0.04)
α	1.25	3.51(0.13)	17.2	105	162	1.03(0.04)

[a] M is the particle multiplicity from the fit of the spectra generated by PACEX simulation.
[b] S is the slope extracted from the ft of the spectra generated by PACEX simulation.
[c] $\bar{\epsilon}$ is the average energy carried away by the particle.
[d] $A = A_{CN} - A_{\text{part}}$.
[e] $U_d = E^* - (BE) - \bar{\epsilon} - \bar{E}_r$, where (BE) is the binding energy of the particle emitted, $\bar{E}_r$ = is the average rotational energy, and $\bar{\epsilon}$ is the average channel energy.
[f] f_w is the correction factor determined using Eq. (7), see text.

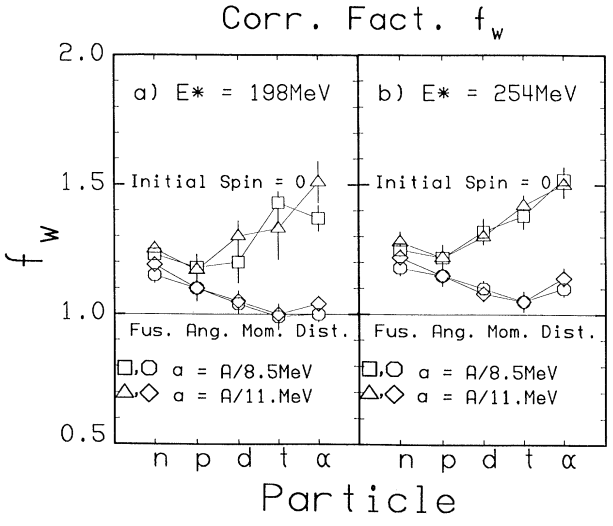

FIG. 2. The whole cascade correction factors f_w deduced from the PACEX simulation of n, p, d, t, and α spectra from the decay of ^{110}Ag at two excitation energies: (a) $E^* = 198$ MeV, (b) $E^* = 254$ MeV. These calculations are made with zero initial spin (triangles and squares) and with a fusion angular momentum distribution (diamonds and circles) for the system ^{10}B + ^{100}Mo. The fusion angular momentum distributions are those of the Bass model, see Table I. The level density parameters used are indicated in the figure.

in the transfer of collective rotational energy to ejectile kinetic energy. This "spin-off energy" inflates the spectra yielding larger slopes and thus smaller correction factors as the ejectile mass increases. This procedure has been used by Hilscher *et al.*[8] for neutron spectra from the reaction 30 MeV/nucleon ^{20}Ne + ^{165}Ho. In Ref. 8, Hilscher *et al.* use the correction factor for a pure neutron cascade without angular momentum, $f_w = 12/11$, first derived by Le Couteur and Lang.[20] Cheynis[9] used evaporation simulations to deduce a correction factor of ~ 1.2 for the same data. This value is consistent with our simulations.

It is instructive to examine the influence of excitation energy "backshifting" and the number of open decay channels on f_w. Part (c) of Table II gives the results of sensitivity tests directed at addressing these two questions. The Gilbert and Cameron[11] shifting was turned on and off and the set of decay channels was limited to n, p, and α particles (the original PACE set).

The variation of the values of f_w due to the backshifting option is similar in magnitude to the statistical error (propagated through from the fitted slope and given in parentheses in Table II). Therefore, for primary excitation energies approaching (or exceeding) 200 MeV, backshifting is of little importance. Undoubtedly, as the excitation energy is decreased, the sensitivity to backshifting increases. Unfortunately, this creates an ambiguity at low energy. The backshift is introduced to account for

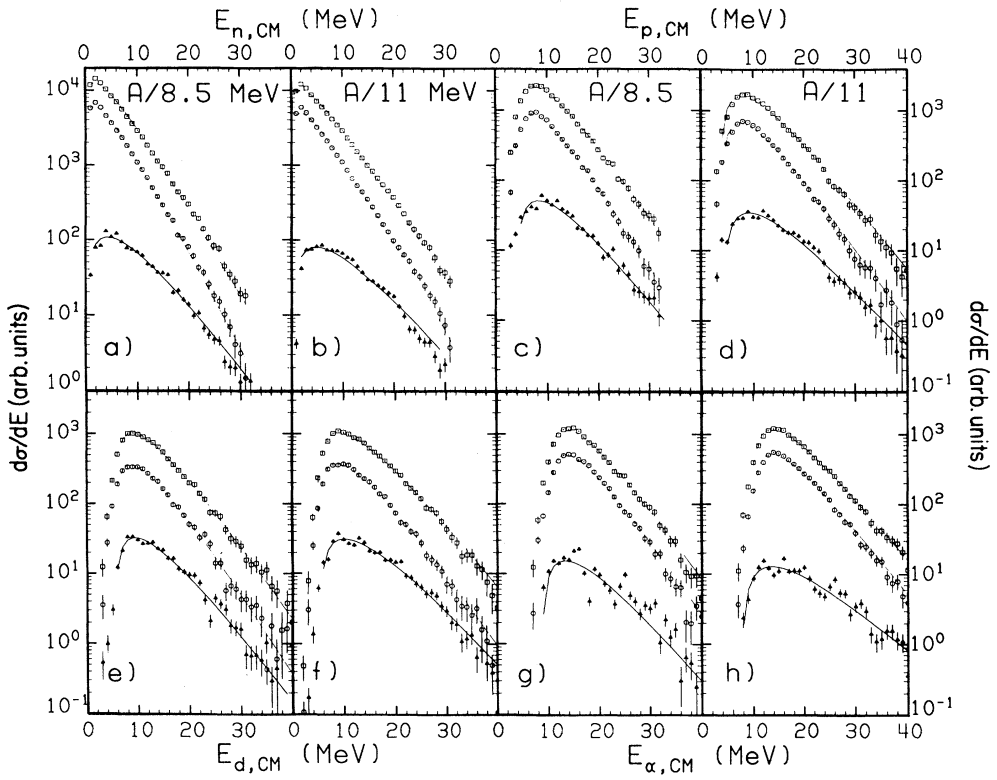

FIG. 3. Calculated whole cascade and difference spectra resulting from the decay of ^{110}Ag at 198 and 253 MeV of excitation energy. In each frame, the spectra corresponding to the higher excitation energy (top), the lower excitation energy (middle) and the difference spectrum (bottom) are shown. The solid curves correspond to the fitted Maxwellian form. (a) and (b) display neutron spectra, (c) and (d) display proton spectra, (e) and (f) display deuteron spectra, and (g) and (h) display α-particle spectra. The level density parameters used are indicated in the figure.

both shell structure and pairing, which melt or at least change with excitation and angular momentum. Therefore, small changes in a at low and moderate excitation energies cannot easily be disentangled from the disappearance of the shell structure or the pairing gap.

The change in f_w introduced by limiting the set of decay channels is also similar in magnitude to the statistical uncertainty. However, this difference will grow with excitation energy. Therefore, while expanding the set of decay channels is of marginal significance at $E^*=200$ MeV (4–5 % in f_w, 8–10 % in a), it is required if reliable results are to be obtained at higher energy.

The second procedure utilizes difference spectra to define a region of excitation energy. Gonin *et al.*[10] have applied this procedure to the decay of ^{160}Yb at 251 and 291 MeV of excitation energy produced by ^{60}Ni+^{100}Mo reactions. An obvious concern one must have about this procedure is that the lower initial E^*-spin distribution is not "genetically" related to that of the parent. (The upper distribution does not produce the lower one.) This concern and the utility of this method to incomplete fusion reactions are discussed in the following sections.

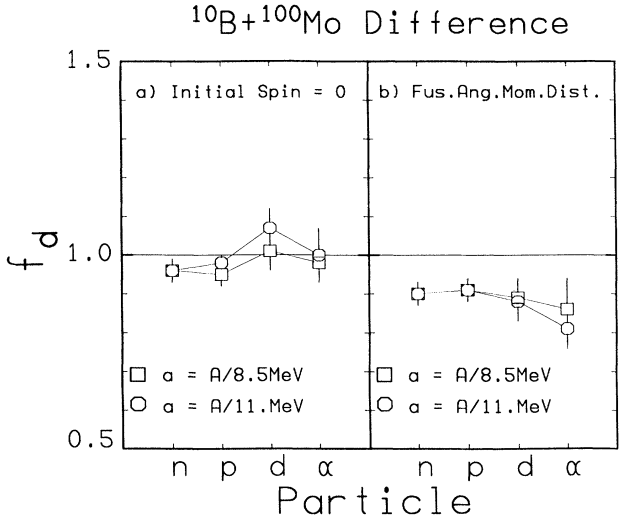

FIG. 4. The correction factors f_d deduced from the difference calculated n, p, d, and α spectra. Those simulations are made with (a) zero initial spin and (b) fusion angular momentum distribution of the system ^{10}B+^{100}Mo.

TABLE III. Difference spectra correction factors for the system $^{10}B+^{100}Mo$.

Part.	S [a] (MeV)	A [b]	U_d [c] (MeV)	$k=A/a$ (MeV)	f_d [d]
		(a) $k=A/a=8.5$ MeV			
Zero initial spin					
n	4.20(0.10)	109	210	9.2(0.5)	0.96(0.03)
p	4.23(0.10)	109	206	9.5(0.5)	0.95(0.03)
α	4.15(0.21)	105	206	8.8(0.9)	0.98(0.05)
d	3.97(0.20)	108	202	8.3(0.9)	1.01(0.05)
Fusion initial angular momentum distribution					
n	4.32(0.10)	109	194	10.5(0.5)	0.90(0.02)
p	4.23(0.13)	109	189	10.3(0.7)	0.91(0.03)
α	4.57(0.40)	105	190	11.5(2.0)	0.86(0.08)
d	4.13(0.15)	108	187	10.0(0.7)	0.93(0.04)
		(b) $k=A/a=11.0$ MeV			
Zero initial spin					
n	4.78(0.10)	109	210	11.9(0.5)	0.96(0.03)
p	4.65(0.10)	109	206	11.4(0.5)	0.98(0.02)
α	4.64(0.30)	105	206	11.0(1.5)	1.00(0.07)
d	4.24(0.20)	108	201	9.7(1.0)	1.07(0.05)
Fusion initial angular momentum distribution					
n	4.93(0.12)	109	193	13.7(0.7)	0.90(0.03)
p	4.83(0.11)	109	190	13.4(0.7)	0.91(0.03)
α	5.50(0.30)	105	187	17.0(2.0)	0.81(0.05)
d	4.94(0.25)	108	184	14.3(1.5)	0.88(0.05)

[a] S is the slope extracted from the fit of the difference spectra generated by PACEX simulation of two excitation energies.
[b] $A=A_{Cn}-A_{\text{part}}$.
[c] $U_d=Ex-(BE)-\bar{\epsilon}-\bar{E}_r$, where $Ex=(E_1^*+E_2^*)/2$, the average excitation energy between $E_1^*=254$, $E_2^*=198$ MeV. (BE) is the binding energy. $\bar{E}_r$=is the average rotational energy and $\bar{\epsilon}$ is the average channel energy.
[d] f_d the correction factor determined using Eq. (7), see text.

The whole cascade and the difference spectra for n, p, d, and α particles for our two test cases are shown in Fig. 3 for the two level density constant values. The fitted values of the slopes, and the mean daughter excitation (calculated from a parent excitation E^* midway between the two initial excitations), and the deduced correction factors are given in Table III. Plotted in Fig. 4 are the correction factors which result from using both zero initial spin and the fusion spin distribution, Figs. 4(a) and 4(b), respectively. While the correction factors are near 1 for the zero inital spin case, they are less than 1 and tend to decrease with ejectile mass for the case with a spin distribution. The relative difference between these calculations is the same as we saw in the "whole chain" calculation in Fig. 2 and the same explanation can be offered here.

The method employing the difference spectra does bring the correction factors much closer to 1 and removes much of channel dependence of the correction factors. In addition some of the sensitivity to the angular momentum distribution is removed. However, correction factors are still required for the treatment of heavy-ion fusion reactions [which will have spin distributions similar to the one used to generate the correction factors plotted in Fig. 4(b)]. Neglecting this correction in our test simulation would result in a 10% inflation of T and therefore, a 20% underprediction of a.

As mentioned at the end of Sec. II A, decreasing the level density constant enhances the emission of particles which are expensive in terms of the excitation energy removed from the compound system. This can be seen in the results of simulations of the test case $^{10}B+^{100}Mo$. For example, comparing the cases with a fusion angular momentum distribution with $E^*=254$ MeV, the simulation with $a=A/8.5$ [see part (a) of Table II] yields a value of the ratio M_d/M_p of 0.47 while the simulation with $a=A/11$ [see part (b) of Table II] yields a value of 0.67. A similar enhancement (30% to 50%) is found for the other cases (different excitation energies and spin distributions). Due to the sensitivity of the channel multiplicities to the value of a, in the next section, we use both the experimental spectral shapes (with the aid of the correction factors) and the experimental multiplicities to study the behavior of the level density constant at high excitation energy.

III. ANALYSIS FROM THE REACTION OF 701 MeV ^{28}Si WITH ^{100}Mo

While the near yrast structure (shell and pairing) and the gamma decay strengths become less important at high energy, additional complications arise. These include uncertainties in the actual primary excitation energy and as just discussed, the number of important decay channels. The proper treatment of the complete reaction evolution would be the best way to deal with the excitation energy distribution. However, in this work, we opt to select events using an experimental observable which restricts the primary excitation energy to a defined region. (It is worth noting that the broad excitation distributions used in this work are better suited to the difference method than those resulting from compound nucleus reactions. This is due to the fact that the upper compound nucleus distribution never decays to anything resembling the initial lower compound nucleus distribution.) The comparison of these selected events to evaporation simulations must then be done on the basis of spectral shapes and particle multiplicities) rather than absolute cross sections.) The second complication mentioned above has been addressed by expanding the number of decay channels in the statistical model code used in the simulations.

The system we have studied is 701 MeV ^{28}Si+^{100}Mo. Evaporation residues were detected in an annular parallel plate avalanche counter spanning 2.1° to 8.1°, charged particles were detected in the Dwarf Ball/Wall system,[21] and neutrons and γ rays were detected in the Spin Spectrometer.[22] Details concerning this experiment can be found in Refs. 23 and 24. The spectrum of residue velocities was divided into six bins which correspond to six energy regions. The excitation energy regions and the primary mass are determined by a linear momentum reconstruction procedure which is described in the preceding paper.[24] Representative spectra, whole chain and difference, from backward angle data are shown in Fig. 5 for protons (top) and deuterons (bottom). To improve the statistics in the difference spectra, data from detectors between 113°–155° have been summed. In addition, the difference spectra are created by bypassing an intermediate bin. The initial excitation energies and primary masses determined from the reconstruction procedure, estimated initial average angular momenta, and the other factors relating to the level density factor determination are listed in Table IV.

The correction factors (both f_d and f_w) are deduced from simulations of the decay of the primary system (mass A_p) with excitation energy E_p^* and an angular momentum distribution with mean value $\bar{I}$. The systems

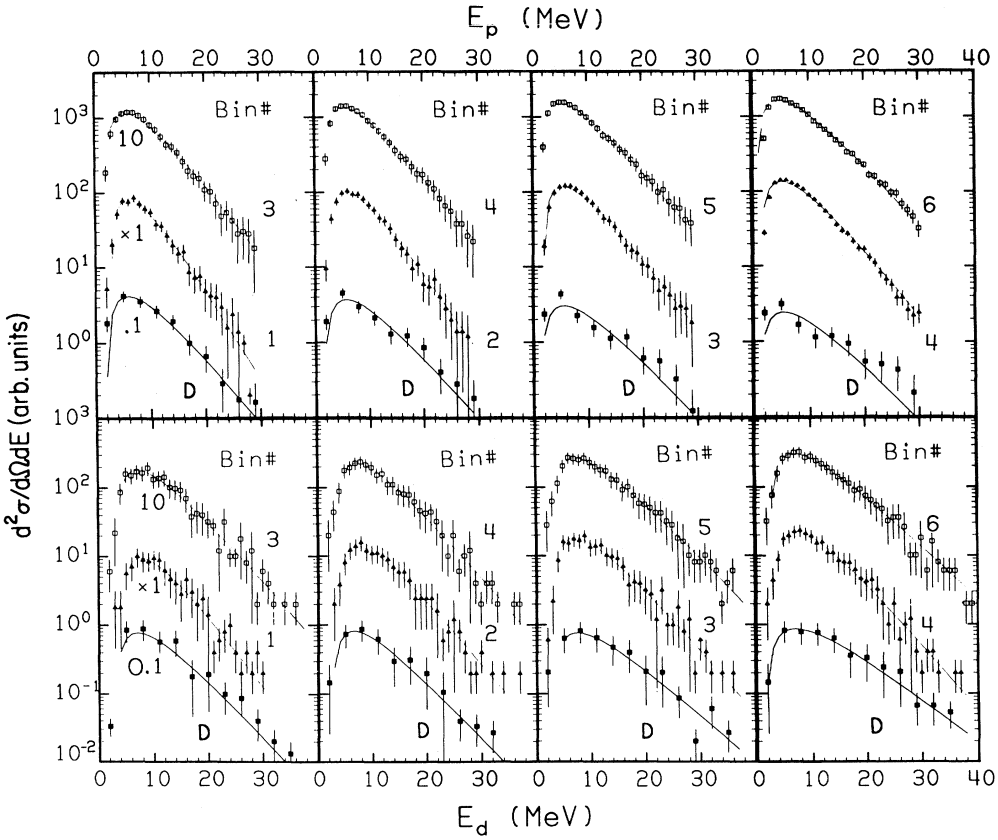

FIG. 5. The experimental proton and deuteron spectra corresponding to six bins in the residue velocities for the reaction 701 MeV ^{28}Si+^{100}Mo are displayed in the top and bottom halves of the figure, respectively. In each frame, the spectra correspond to the higher excitation energy (top), the lower excitation energy (middle) and the difference spectrum (bottom) are shown. The parameters for each bin including the fitted slope and extracted level density constant are given in Table IV.

and parameters used to simulate the decay of the primary compound systems corresponding to the six residue velocity bins are given in lines (4)–(9) of Table I. The preceding paper[24] describes how E_p^* and A_p are deduced. Our estimates of the angular momentum distribution requires some additional comments.

As mentioned in Ref. 24, the γ-ray multiplicity is independent of residue velocity. This is not surprising since γ rays remove only a small portion of the total spin. In fact, the simulations indicate one α particle can remove more spin than the entire γ-ray cascade. We therefore have no direct measure of the initial spin distributions. We have therefore relied on the sum-rule model of Wilczyński[25] for an estimate of the l-wave distributions

TABLE IV. Level density parameter results for the system 701 MeV ^{28}Si + ^{100}Mo.

Bin	E_p^* [a] (MeV)	A_p	$\bar{I}$ ($\hbar$)	S [b] (MeV)	U_d [c] (MeV)	f_w [d]	$k = A/a$ (MeV)
			(a) Whole spectra				
Proton							
6	405	121(2)	48.8	4.88(0.10)	362.(29)	1.17	10.8(1.5)
5	372	119(2)	47.7	4.60(0.08)	334.(27)	1.17	10.2(1.4)
4	316	114(1)	36.1	4.40(0.07)	283.(23)	1.16	10.4(1.3)
3	260	110(1)	27.2	4.12(0.07)	233.(19)	1.20	11.4(1.4)
2	200	107(1)	21.1	3.78(0.10)	176.(14)	1.19	12.2(1.7)
1	158	105(1)	18.2	3.29(0.08)	136.(11)	1.10	10.0(1.2)
Deuteron							
6	405	121(2)	48.8	5.60(0.14)	352.(28)	1.06	11.9(1.7)
5	372	119(2)	47.7	5.08(0.14)	325.(26)	1.08	10.8(1.6)
4	316	114(1)	36.1	4.60(0.10)	276.(22)	1.12	10.8(1.4)
3	260	110(1)	27.2	4.54(0.16)	227.(19)	1.19	13.9(2.2)
2	200	107(1)	21.1	4.12(0.11)	168.(14)	1.11	13.1(1.9)
1	158	105(1)	18.2	3.73(0.17)	128.(10)	1.06	12.6(2.3)
Triton							
6	405	121(2)	48.8	6.80(0.20)	348.(28)	1.10	19.0(3.0)
5	372	119(2)	47.7	5.50(0.16)	323.(26)	1.07	12.4(1.9)
4	316	114(1)	36.1	5.00(0.20)	272.(23)	1.14	13.3(2.3)
3	260	110(1)	27.2	4.90(0.20)	224.(18)	1.18	16.0(2.8)
2	200	107(1)	21.1	4.20(0.20)	168.(14)	1.17	15.0(2.8)
1	158	105(1)	18.2	4.00(0.17)	128.(10)	1.14	16.6(3.0)
Alpha							
6	405	121(2)	48.8	5.50(0.12)	360.(29)	1.10	12.0(1.7)
5	372	119(2)	47.7	5.11(0.10)	330.(27)	1.12	11.4(1.6)
4	316	114(1)	36.1	5.00(0.10)	281.(23)	1.17	13.4(1.7)
3	260	110(1)	27.2	4.80(0.12)	231.(19)	1.22	15.7(2.2)
2	200	107(1)	21.1	4.60(0.10)	173.(14)	1.22	18.8(2.5)
1	158	105(1)	18.2	3.90(0.12)	134.(11)	1.16	15.4(2.4)
			(b) Difference spectra				
Proton							
6-4	405	121(2)	48.8	5.40(0.23)	318.(26)	1.00	11.0(2.0)
5-3	372	119(2)	47.7	5.20(0.20)	274.(22)	0.95	10.5(1.8)
4-2	316	114(1)	36.1	4.80(0.10)	225.(18)	0.97	10.9(1.5)
3-1	260	110(1)	27.2	4.40(0.15)	179.(15)	0.99	11.6(1.7)
Deuteron							
6-4	405	121(2)	48.8	6.60(0.25)	308.(25)	0.95	15.2(3.0)
5-3	372	119(2)	47.7	5.70(0.21)	266.(22)	0.87	10.8(1.7)
4-2	316	114(1)	36.1	4.80(0.10)	217.(18)	0.93	10.3(1.4)
3-1	260	110(1)	27.2	4.60(0.10)	174.(15)	0.94	11.6(1.7)

[a] E_p^* is the excitation energy of the primary residue (A_p) deduced from the linear momentum reconstruction.

[b] S is the slope of the fitted difference spectra. The statistical temperature is $S * f_i$.

[c] $U_d = Ex - (BE) - \bar{\epsilon} - \bar{E}_r$, where $Ex = (E_{p1}^* + E_{p2}^*)/2$, the average excitation energy between E_{p1}^* and E_{p2}^*. (BE) is the binding energy and $\bar{\epsilon}$ is the average channel energy. $\bar{E}_r = \bar{I}^2/2\mathcal{I}$ = rotational energy, where I is the average angular momentum estimated from the sum-rule model and $\mathcal{I}$ = spherical moment of inertia calculated with $r_0 = 1.4$ fm.

[d] f_d and f_w are the correction factors determined using Eq. (7), see text.

contributing to an incomplete fusion channel. For the purpose of the sum-rule calculation, we assumed that the remainder of the projectile $(100+28-A_p)$ continues forward as one fragment. The l-wave distributions increase in mean value as the mass of the nonfusing fragment increases. However, the transferred spin distribution, which is calculated by weighting the probability of a given l wave by the fractional mass transfer, decreases in mean value as the mass of the nonfusing fragment increases. As a result, the whole chain correction factors f_w, initially increase with excitation energy [bins 1–3 in Table IV) and then decrease, contrary to the trend expected, due to the influence of the higher spin values (bins 4–6 in Table IV, see also Fig. 2).

While the procedure discussed above is reasonable, we have no means to verify it. Therefore we only have confidence in the results that are rather insensitive to the spin distribution, namely, those derived from the lightest mass ejectiles.

The last column of Table IV lists the level density constant denominator $k = A/a$ as determined from the whole cascade in part (a), and from the difference method in part (b). Due to the uncertainty introduced by the spin distribution, we have focused our attention on the results deduced from the p and d data. The values of k range from 10 to 15 MeV, but most are in the range of 10–11 MeV. There is no systematic trend with excitation energy of the residual which varies from slightly below 150 MeV to slightly more than 350 MeV (see column 6 in Table IV). These excitation energies correspond to statistical temperatures in the range of approximately 3.5 to 5.5 MeV.

The constants deduced from both spectral shapes (whole chain and difference) are consistent with each other, but are inconsistent with those deduced for nuclei in the same Z and A range with low to moderate excitation. (See Fig. 1 and the associated discussion in Sec. III). This analysis suggests a substantial reduction in a as the temperature changes from less than 2.5 to more than 3.5 MeV. The simulations, the related corrections, and our focus on the p and d data convince us that this result is not significantly influenced by uncertainties in the angular momentum distributions or the influence of backshifting or a limited set of decay channels. An obvious concern, is the absolute excitation energy. This uncertainty is estimated in the previous work[24] to be in the worst case of the order of 15%, see Fig. 13 of Ref. 24. Therefore, there is little doubt that in order to reproduce the shapes of spectra by adjusting only the level density parameter that it must be reduced by approximately 30%.

As shown at the end of the previous section, the multiplicities are also sensitive to the value of a. The evaporative multiplicities of all particles associated with each residue velocity bin are given in Table II of Ref. 24. We have found that the multiplicities of n, p, and α particles calculated with values of k between 6 and 11 are within 30% of the experimental values. On the other hand, the deuteron and triton multiplicities are overpredicted by large factors when large values of k are used. This can be seen in Fig. 6 where the ratios M_d/M_p and M_t/M_p are shown in Figs. 6(a) and 6(b), respectively, for the data and simulations with three different values of k (6, 8.5, and 11 MeV). The experimental values of M_d/M_p and M_t/M_p (represented by stars in Fig. 6) vary from 0.13 to 0.23 and 0.04 to 0.10, respectively, both increasing with increasing excitation energy. However, to get values of these ratios in this range from the simulations, the value k must be close to or even less than the values appropriate for low excitation energy $k<8$, see Sec. II A. Therefore, if one tries to deduce a from multiplicities rather than the slopes of spectra the conclusion would be that a must be large, $a > A/8.5$. We should mention that we have tried both energy and energy independent optical model parameters, eliminating the real part of the optical potential, and changing the charge of the emitting system within reasonable limits. Under no conditions can we reproduce the small values of M_d/M_p and M_t/M_p with large values of k $(k>10)$. Friedman has verified this point using a statistical model code.[26]

IV. DISCUSSION

Our results using the slopes of the evaporative spectra are in qualitative agreement with the experimental work done by the Texas A&M group.[10] Our numerical results for k based solely on the slopes are in quantitative agreement with the highest excitation energy results of the

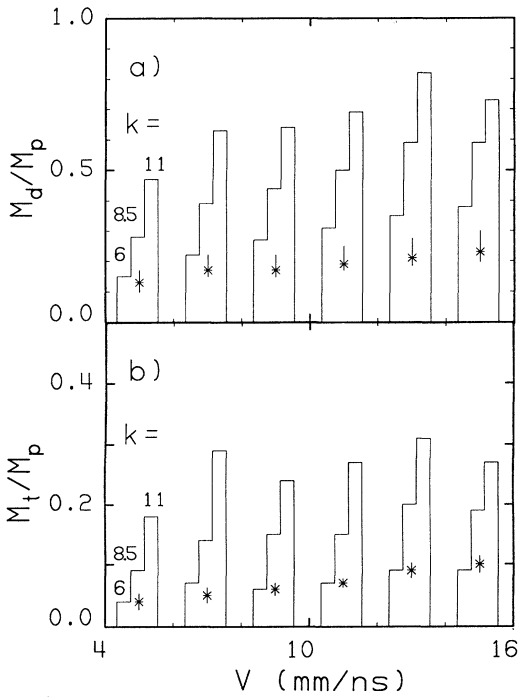

FIG. 6. The ratio (a) M_d/M_p and (b) M_t/M_p are plotted for the experimental (stars) and the simulations (histograms) with three different values of k, for the six bins in residue velocity. The values of k used in the simulations are indicated on the corresponding step of the histogram. The ratios increase as the value of k increases. The experimental error bars are indicated. The asymmetric error bars, corresponding to the larger values of M_d, result from the possibility of confusing low-energy deuterons and protons, see Ref. 24.

work reported by Wada *et al.* for the $^{32}S+Ag$ system while they are slightly lower than those reported by Gonin *et al.* for the $^{60}Ni+^{100}Mo$ system. We suspect that this is due to the expected dependence of k on the total mass of the system. Based on the work of Tõke and Swiatecki,[2] one would expect the lighter nuclei, which have a larger fraction of the density unsaturated, to have smaller values of k.

It is perhaps somewhat surprising that our results using the slopes of the evaporation spectra indicate that the level density parameter does not change significantly in the temperature range 3.5 to 5.5 MeV, while they do imply a large change from the values at slightly lower temperatures. However, this is exactly what the theory predicts.[5–7] The nucleon effective mass loses the bulk of the enhancement, due to the coupling of surface vibrations, at rather low temperature. While the effective mass continues to change with temperature, the relevant energy scale is of the order of the Fermi energy and therefore little change is expected over the next few MeV span.[3]

However, in light of the overprediction of the yield of expensive particles (Such as deuterons and tritons) for large values of k, one cannot be confident of the conclusion that the level density does decrease with excitation energy. In fact, the nature of our results are such that one must suspect processes which enhance high kinetic energy particle emission without enhancing the emission of "expensive" particle types. The level density constant is unable to do this because it only deals with the excitation energy of the daughter and cannot distinguish between the emission of a proton with large kinetic energy and the emission of a deuteron or triton of lower kinetic energy but which leaves the daughter with the same excitation energy. We are therefore led to suspect a general increase of the transmission coefficients for the emission of high-energy particles from highly excited nuclei or simply a failure of the statistical model.

In summary, we have used light particle emission from an incomplete fusion reaction in an attempt to study the level density parameter in the range of 160 to 400 MeV of excitation energy in nuclei in the mass region $A \sim 110$. The energy spectra, differences between energy spectra, and particle multiplicities were used in this effort. Extensive statistical model calculations served as a guide to how the shapes of particle spectra can be related to the level density parameter. The shape of the evaporation spectra imply a decrease in the level density parameter, a conclusion reached by others. However, the comparison of the particle multiplicities to the evaporation simulations do not support this conclusion.

ACKNOWLEDGMENTS

We would like to acknowledge discussions with Professor W. Dickhoff, Professor J. Wambach, and Professor W. Friedman. This work was supported in part by the U.S. Department of Energy under Contract Nos. DE-FG02-87ER40316 and DE-FG02-88-ER40406. Oak Ridge National Laboratory is operated by Martin Mareitta Energy Systems, Inc. under Contract No. DE-AC05-84OR21400 with the U.S. Department of Energy.

*Permanent address: Institute of Physics, Jagellonian University of Kraków, Poland.

[1] A. Bohr and B. R. Mottelson, *Nuclear Structure* (Benjamin, New York, 1969), Vol. 1.

[2] J. Tõke and W. J. Swiatecki, Nucl. Phys. **A372**, 141 (1981).

[3] M. Prakash, J. Wambach, and Z. Y. Ma, Phys. Lett. **128B**, 141 (1983).

[4] A. Ramos, A. Polls, and W. H. Dickhoff, Nucl. Phys. **A503**, 1 (1989).

[5] R. W. Hasse and P. Schuck, Phys. Lett. B **179**, 313 (1986).

[6] P. F. Bortignon and C. H. Dasso, Phys. Lett. B **189**, 381 (1987).

[7] S. Shlomo and J. B. Natowitz, Texas A&M Report No. 90-08, 1990 (unpublished).

[8] D. Hilscher, H. Rossner, A. Gamp, U. Jahnke, B. Cheynis, B. Chambon, D. Drain, C. Pastor, A. Giorni, C. Morand, A. Dauchy, P. Stassi, and G. Petitt, Phys. Rev. C **36**, 208 (1987).

[9] B. Cheynis, thesis, Institut de Physique Nucléaire, Université Claude Bernard, Lyon, 1987.

[10] G. Nebbia, K. Hagel, D. Fabris, Z. Majka, J. B. Natowitz, R. P. Schmitt, B. Sterling, G. Mouchaty, G. Berkowitz, K. Strozewski, G. Viesti, P. L. Gonthier, B. Wilkins, M. N. Namboodiri, and H. Ho, Phys. Lett. B **176**, 20 (1986); M. Gonin, L. Cooke, K. Hagel, Y. Lou, J. B. Natowitz, R. P. Schmitt, B. Srivastava, W. Turmel, H. Utsunomiya, R. Wada, B. Fornal, G. Naardelli, G. Nebbia, G. Viesti, R. Zanon, G. Prete, P. Gonthier, and B. Wilkins, *ibid.* **217**, 406 (1989); R. Wada, D. Fabris, K. Hagel, G. Nebbia, Y. Lou, M. Gonin, J. B. Natowitz, R. Billerey, B. Cheynis, A. Demeyer, D. Drain, D. Guinet, C. Pastor, L. Vagneron, K. Zaid, J. Alarja, A. Giorni, D. Heuer, C. Morand, B. Viano, C. Mazur, C. Ngô, S. Leray, R. Lucas, M. Ribrag, and E. Tomasi, Phys. Rev. C **39**, 497 (1989).

[11] A. Gilbert and A. G. W. Cameron, Can. J. Phys. **43**, 1446 (1965).

[12] W. Dilg, W. Schantl, H. Vonach, and M. Uhl, Nucl. Phys. **A217**, 269 (1973).

[13] J. R. Huizenga and L. G. Moretto, Annu. Rev. Nucl. Sci. **22**, 427 (1972).

[14] J. Galin, B. Gatty, D. Guerreau, C. Rousset, U. C. Schlotthauer-Voos, and X. Tarrago, Phys. Rev. C **9**, 1113,1126 (1974).

[15] Code PACEX, N. G. Nicolis and J. R. Beene (unpublished); extended version of the code PACE, A. Gavron, Phys. Rev. C **21**, 230 (1980).

[16] D. W. Lang, Nucl. Phys. **77**, 545 (1966).

[17] R. Bass, Nucl. Phys. **A231**, 45 (1974).

[18] A. J. Sierk, Phys. Rev. C **33**, 2039 (1986).

[19] D. G. Sarantites, C. Baktash, N. G. Nicolis, G. Garcia-Bermudez, V. Abenante, J. R. Beene, N. R. Johnson, M. L. Halbert, D. C. Hensley, F. K. McGowan, H. C. Griffin, I. Y. Lee, Z. Majka, M. A. Riley, T. M. Semkow, D. W. Stracener, and A. Virtanen, Phys. Rev. Lett. **64**, 2129 (1990).

[20]K. J. Le Couteur and D. W. Lang, Nucl. Phys. **13**, 32 (1959).
[21]D. W. Stracener, D. G. Sarantites, L. G. Sobotka, J. Elson, J. T. Hood, Z. Majka, V. Abenante, A. Chbihi, and D. C. Hensley, Nucl. Instrum. Methods A **294**, 485 (1990).
[22]M. Jääskeläinen, D. G. Sarantites, R. Woodward, F. A. Dilmanian, J. T. Hood, R. Jääskeläinen, D. C. Hensley, M. L. Halbert, and J. H. Barker, Nucl. Instrum. Methods **204**, 385 (1983).
[23]L. G. Sobotka, Z. Majka, D. G. Sarantites, D. W. Stracener, V. Abenante, T. M. Semkow, D. C. Hensley, J. R. Beene, and M. L. Halbert, *Proceedings of the Symposium on Nuclear Dynamics and Nuclear Disassembly,* Dallas, Texas, 1989 (World Scientific, Singapore, 1989), p. 67.
[24]A. Chbihi, L. G. Sobotka, Z. Majka, D. G. Sarantites, D. W. Stracener, V. Abenante, T. M. Semkow, N. G. Nicolis, D. C. Hensley, J. R. Beene, and M. L. Halbert, Phys. Rev. C **43**, 652 (1991), the preceding paper.
[25]J. Wilczyński, K. Siwek-Wilczyńska, J. van Driel, S. Gonggrijp, D. C. J. M. Hageman, R. V. F. Janssens, J. Lukasiak, R. H. Siemssen, and S. Y. van der Werf, Nucl. Phys. **A373**, 109 (1982).
[26]This result has been verified by Professor W. Friedman using his statistical model code, private communication. While his calculations produced different absolute multiplities than our calculations, the small experimental isotope ratios also could not be reproduced with any reasonable set of parameters corresponding to a large value of k.